Electronic Supplementary Material (ESI) for RSC Advances.

Bimetallic Schiff base complexes for stereoselective polymerisation of racemic-lactide and copolymerisation of racemic-lactide with ε-caprolactone

Zhiqiang Sun, Ranlong Duan, Jingwei Yang, Han Zhang, Shuai Li, Xuan Pang*,

Wenqi Chen and Xuesi Chen

Key Laboratory of Polymer Ecomaterials, Changchun Institute of Applied Chemistry,

Chinese Academy of Sciences, Changchun 130022, China

*Corresponding author. E-mail: xpang@ciac.ac.cn

Tel: +86-431-85262197 Fax: +86-431-85262933

Supporting information

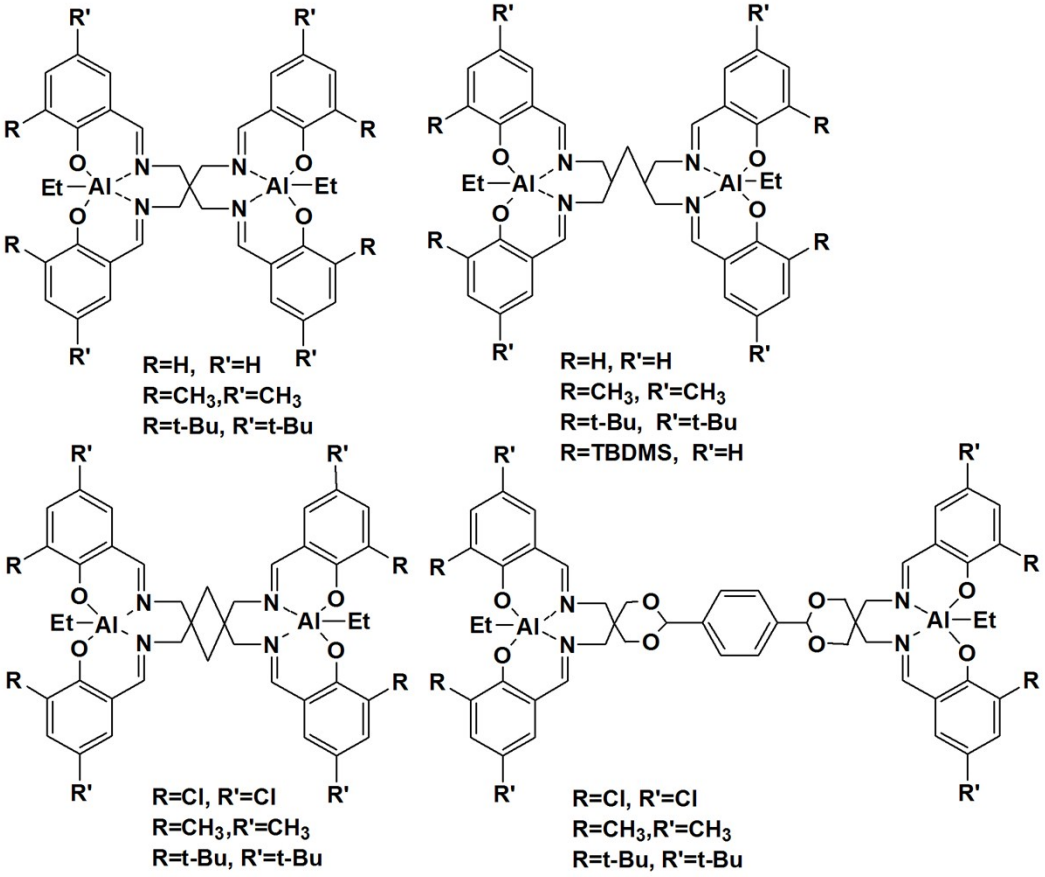

Scheme S1. Bimetallic aluminum salen complexes for ROP of LA and ε-CL reported in our previous work.

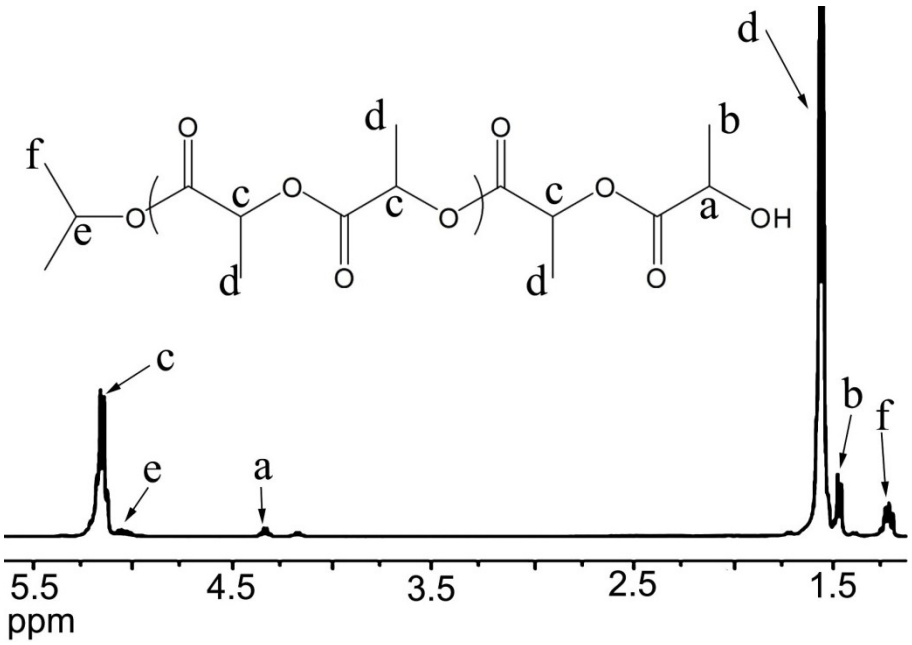

Figure S1.[1]H NMR spectrum of oligomers of rac-LA obtained at a low monomer-to-initiator ratio [rac-LA]:[**1a**]:[iso-propanol]=25:1:2.

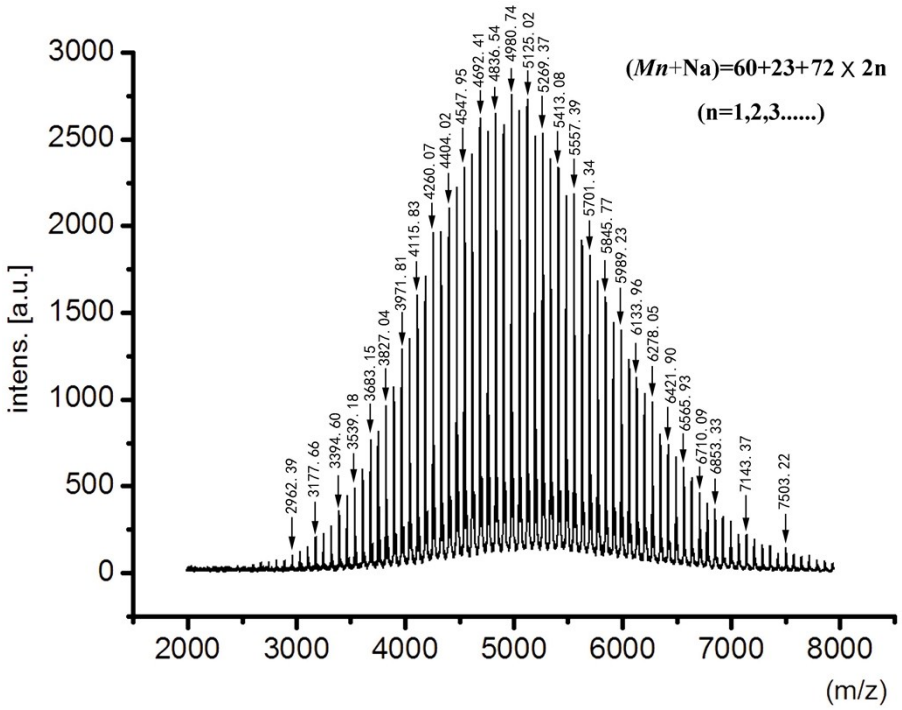

Figure S2. MALDI-TOF of oligomer of poly(rac-LA).

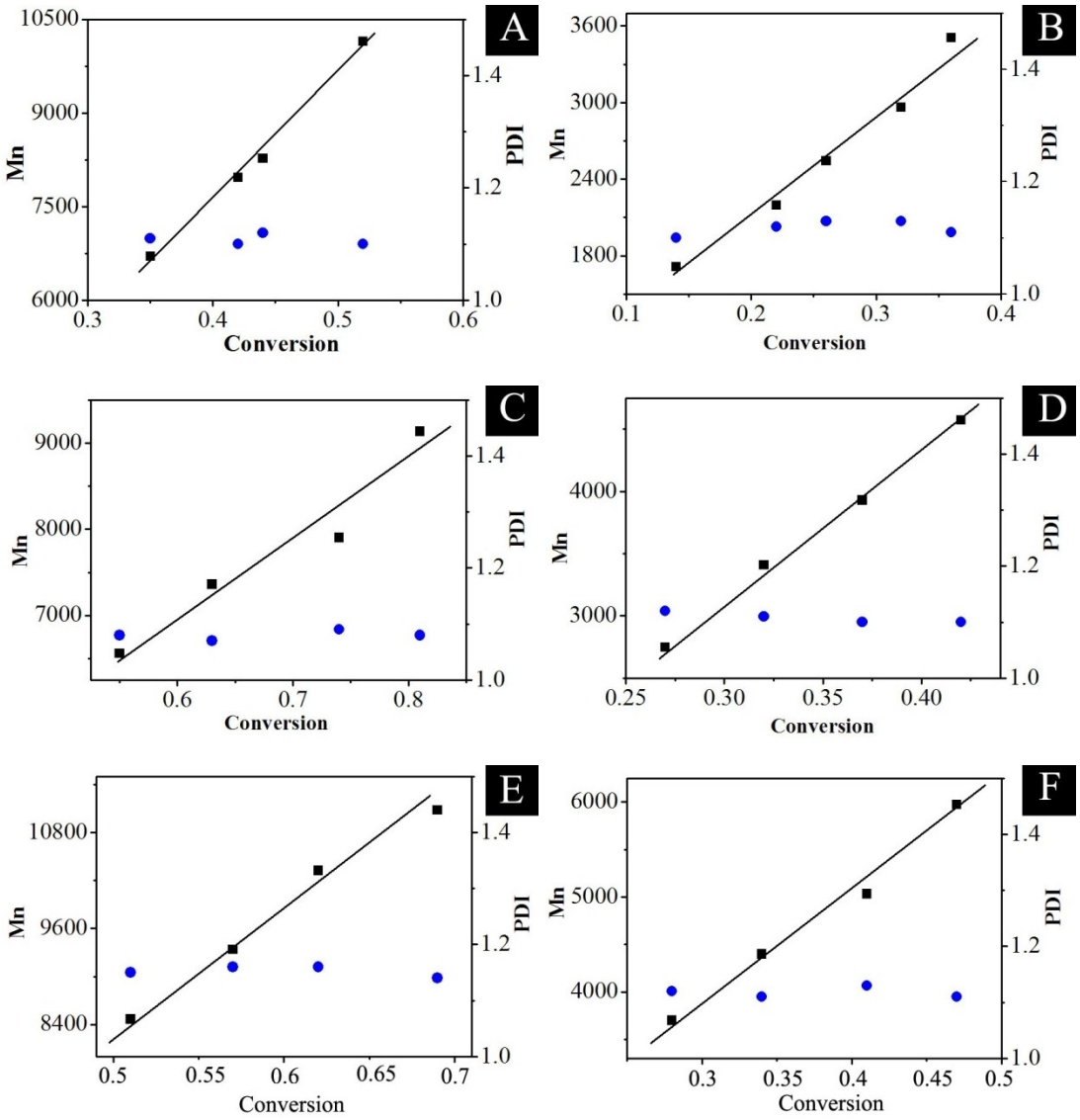

Figure S3. Plots of PLA Mn and PDI (Mw/Mn) as a function of rac-LA conversion using complex (A)1a, (B)2a, (C)3a, (D) 4a, (e) 5a and (F) 6a, T=70℃, [LA]/[Cat]=200:1.

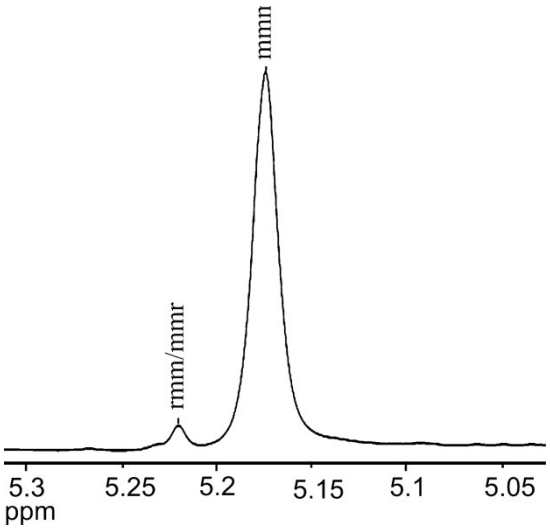

Figure S4. Methine region of homonuclear decoupled ^{1}HNMR spectra of PLA materials using complex **1a**.

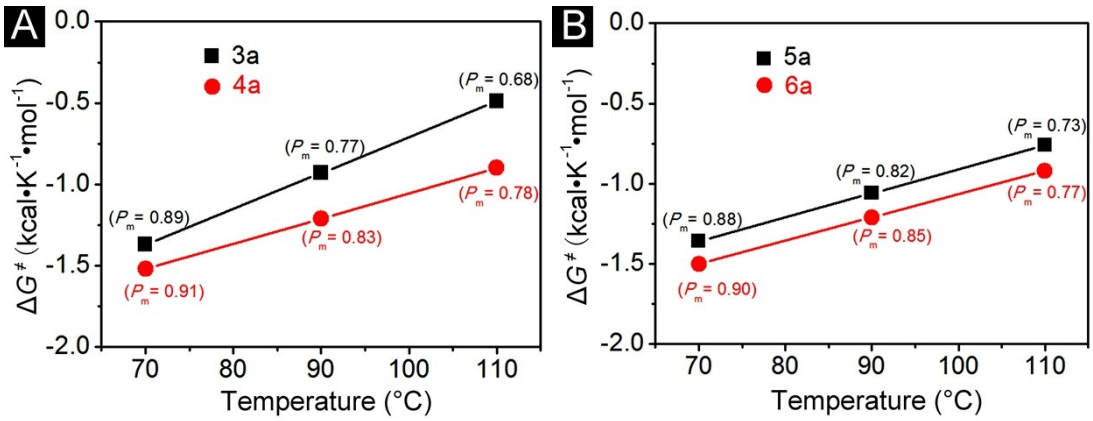

Figure S5. $\Delta G^{\neq}$ values between homo-propagation and cross-propagation for **3a-4a (A)** and **5a-6a (B)** at different temperature.

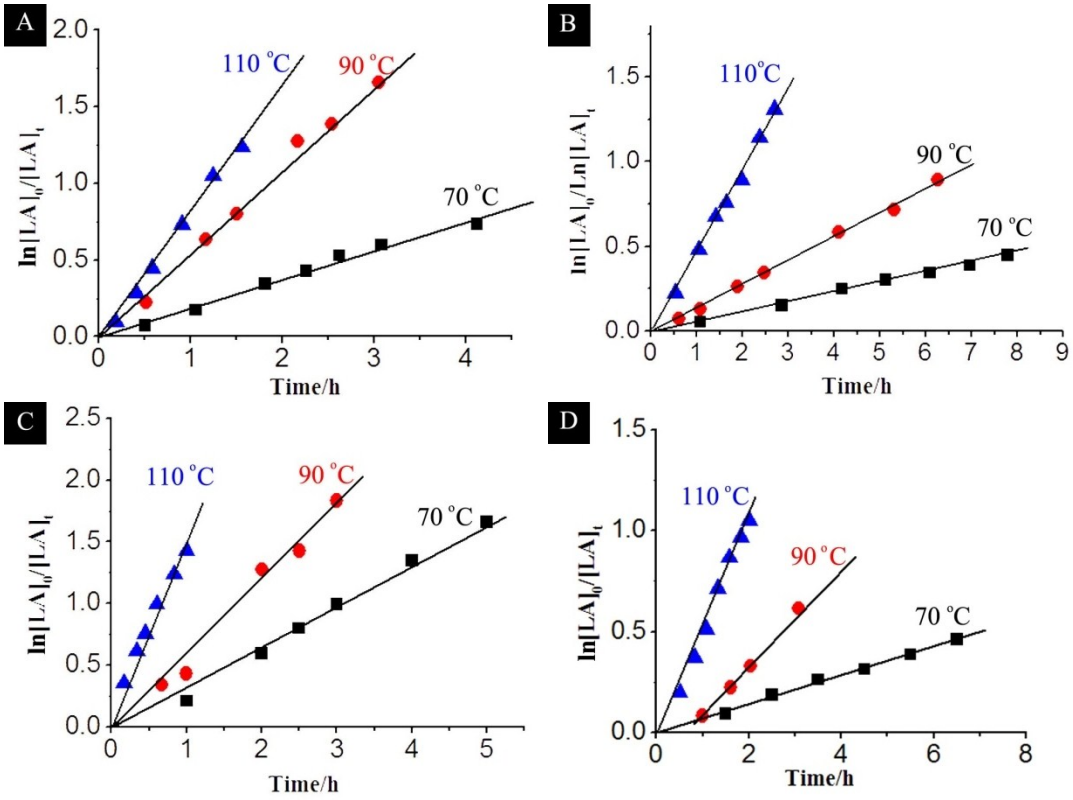

Figure S6. Kinetic plots for ROP of *rac*-LA at different temperature by applying **1a-4a**/iso-propanol as catalyst/initiator in toluene with $[LA]_0$ = 0.5 mol L^{-1}.

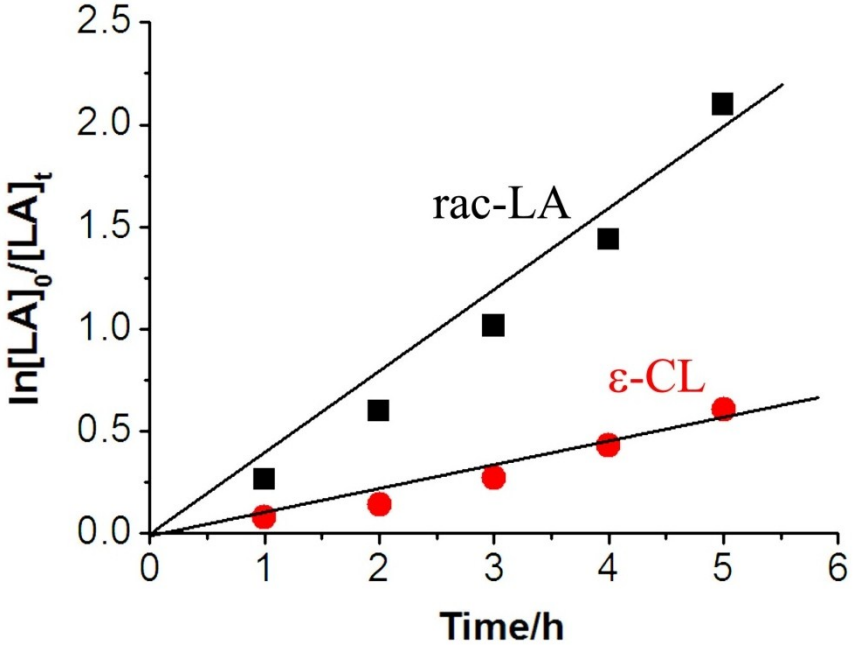

Figure S7. Kinetics of the rac-LA: ε-CL (50:50) copolymerisation using **1a** at 90 °C, $[M]_0/[Cat] = 200$.

Figure S8-(1-6). ^{1}H NMR spectrum of $\mathbf{L^1}$ -$\mathbf{L^6}$.

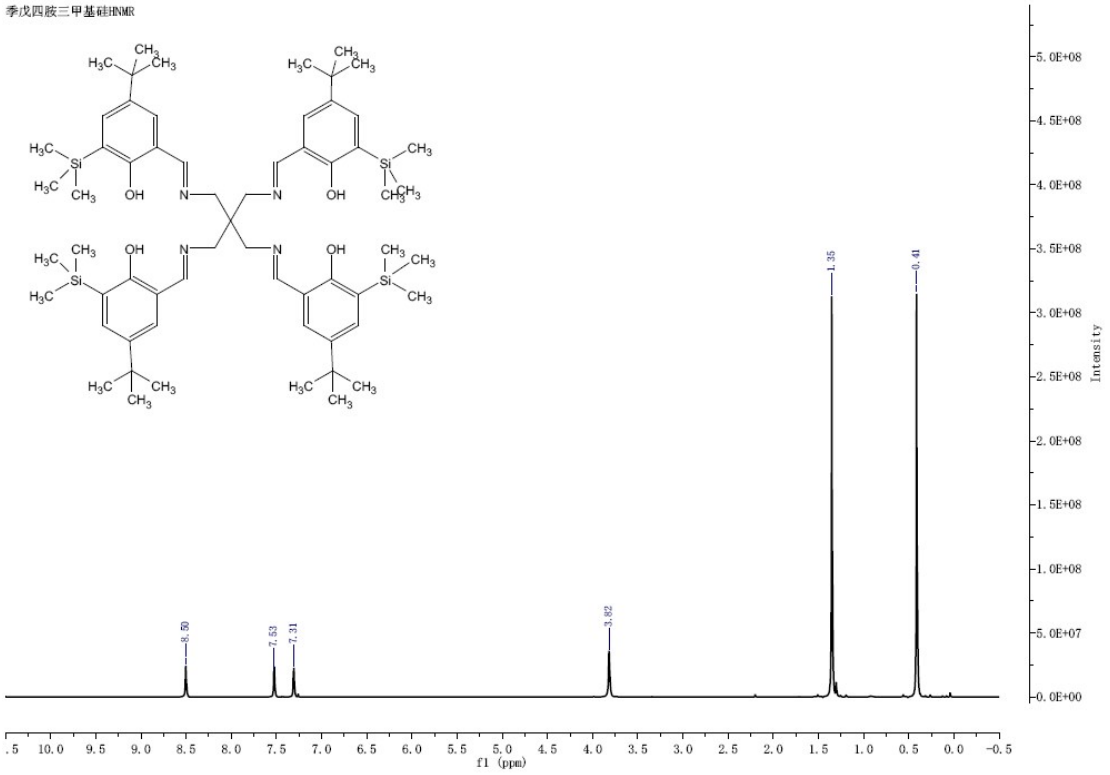

Figure S8-(1). ^{1}H NMR spectrum of $\mathbf{L^1}$.

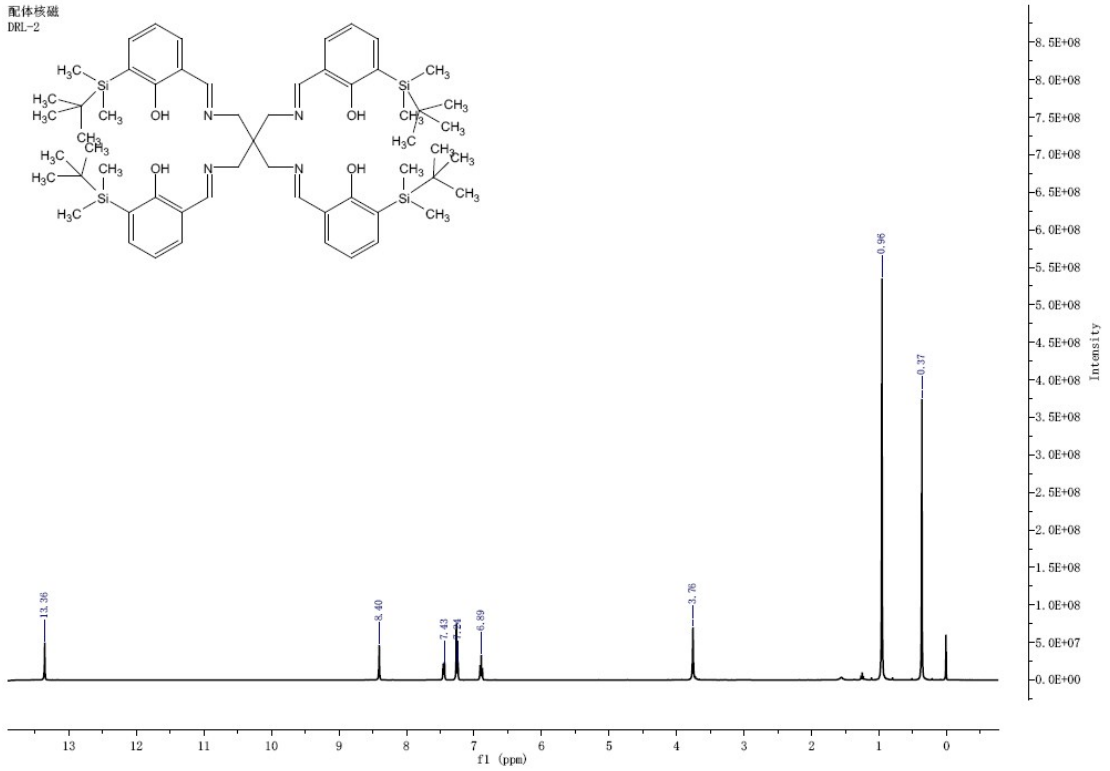

Figure S8-(2). ^{1}H NMR spectrum of $\mathbf{L^2}$.

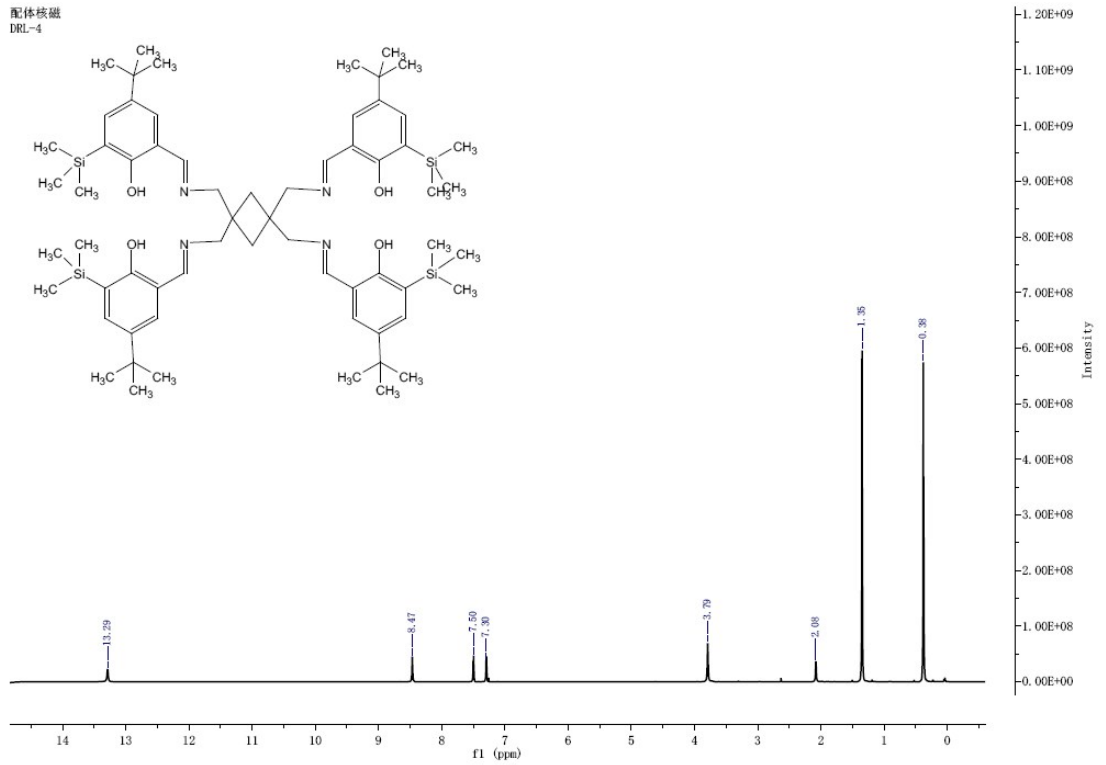

Figure S8-(3). ^{1}H NMR spectrum of **L^{3}**.

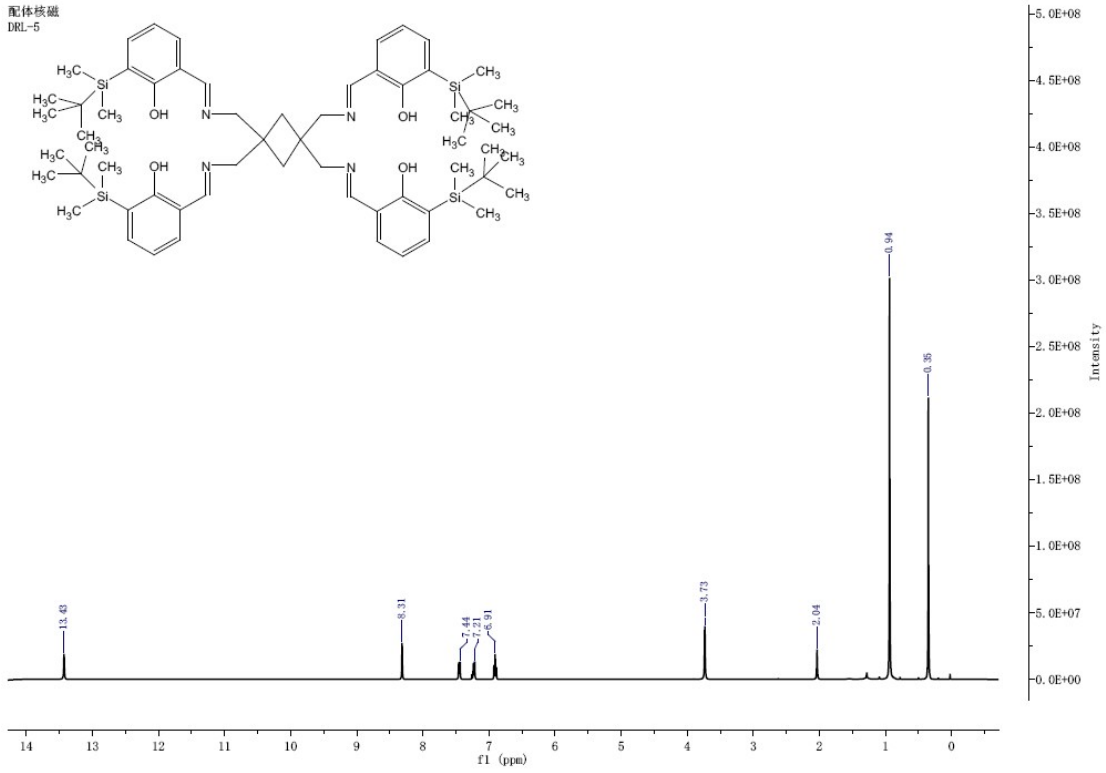

Figure S8-(4). ^{1}H NMR spectrum of **L^{4}**.

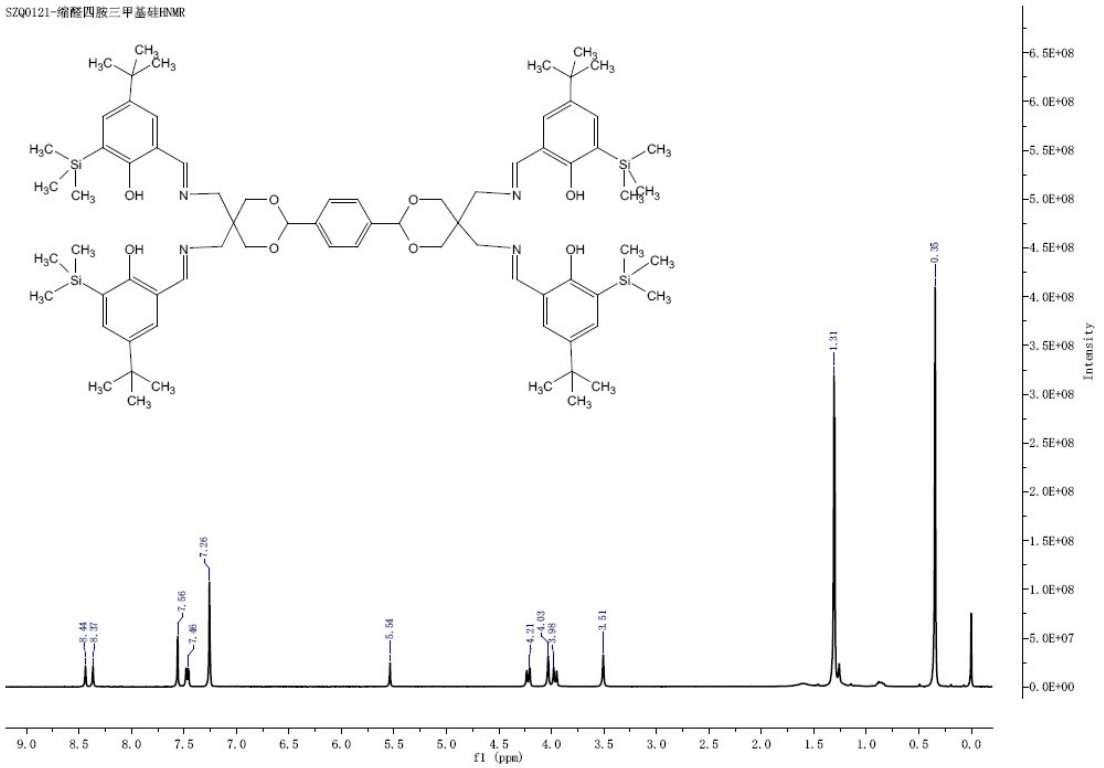

Figure S8-(5). ^{1}H NMR spectrum of **L^{5}**.

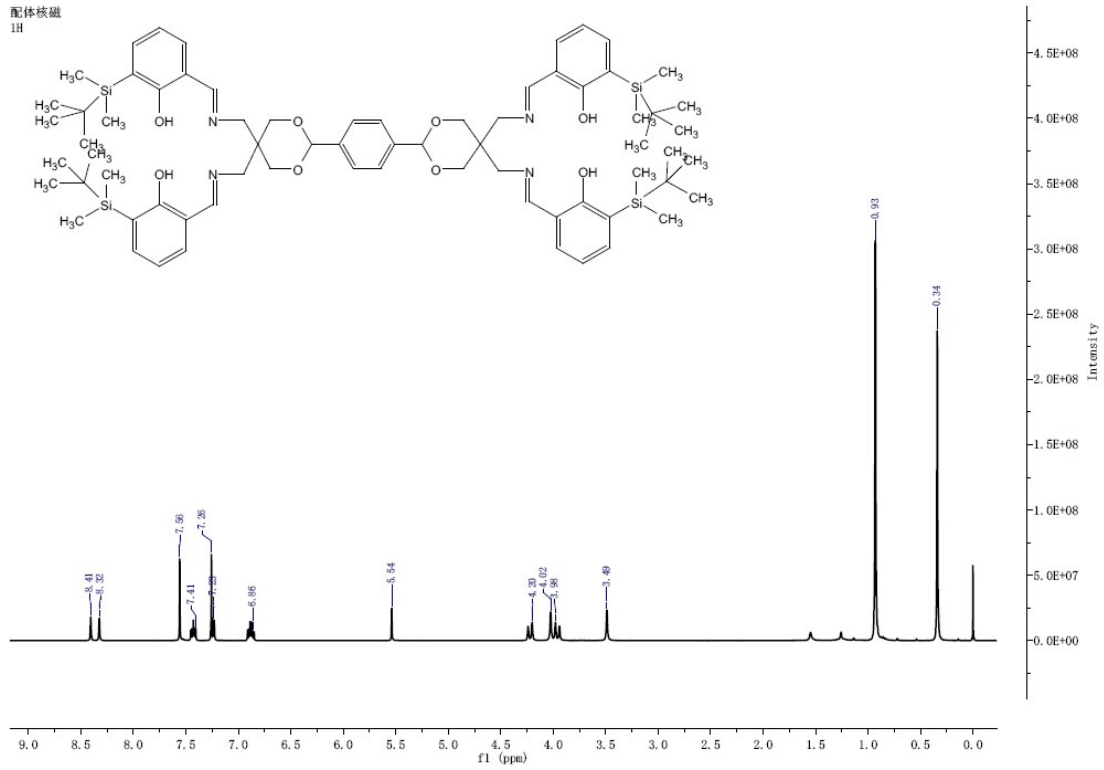

Figure S8-(6). ^{1}H NMR spectrum of **L^{6}**.

Figure S9-(1-6). ^{13}C NMR spectrum of $\mathbf{L^1}$ -$\mathbf{L^6}$.

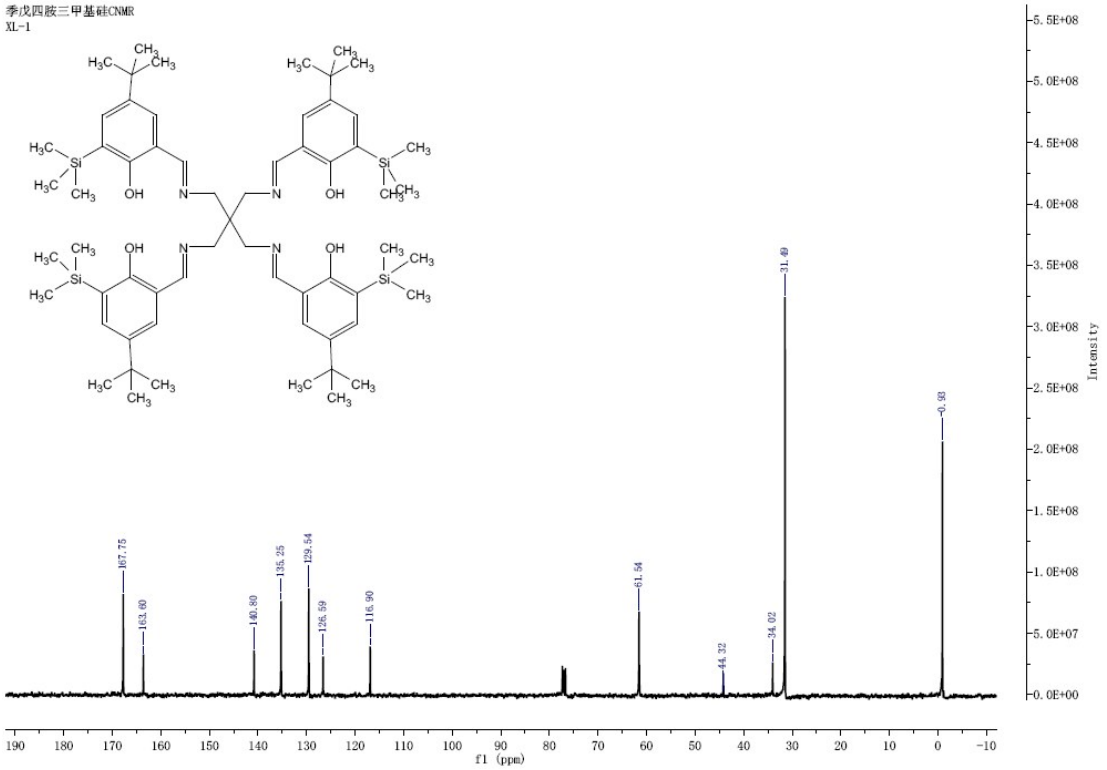

Figure S9-(1). ^{13}C NMR spectrum of $\mathbf{L^1}$.

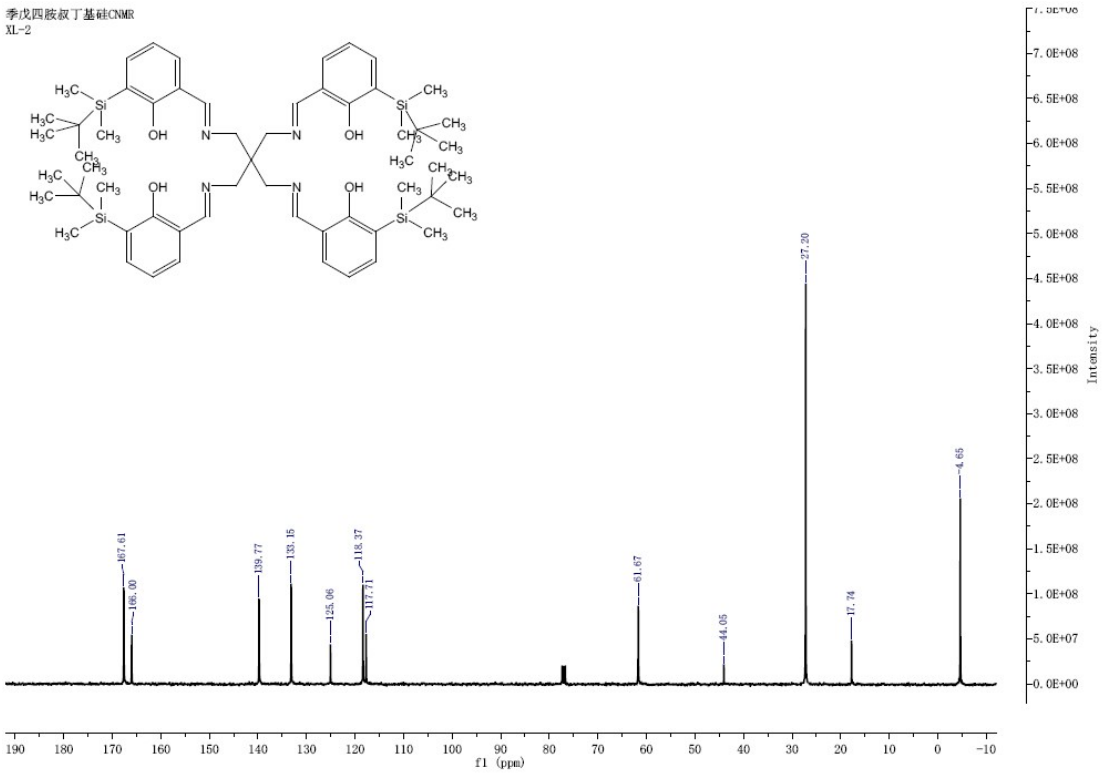

Figure S9-(2). ^{13}C NMR spectrum of $\mathbf{L^2}$.

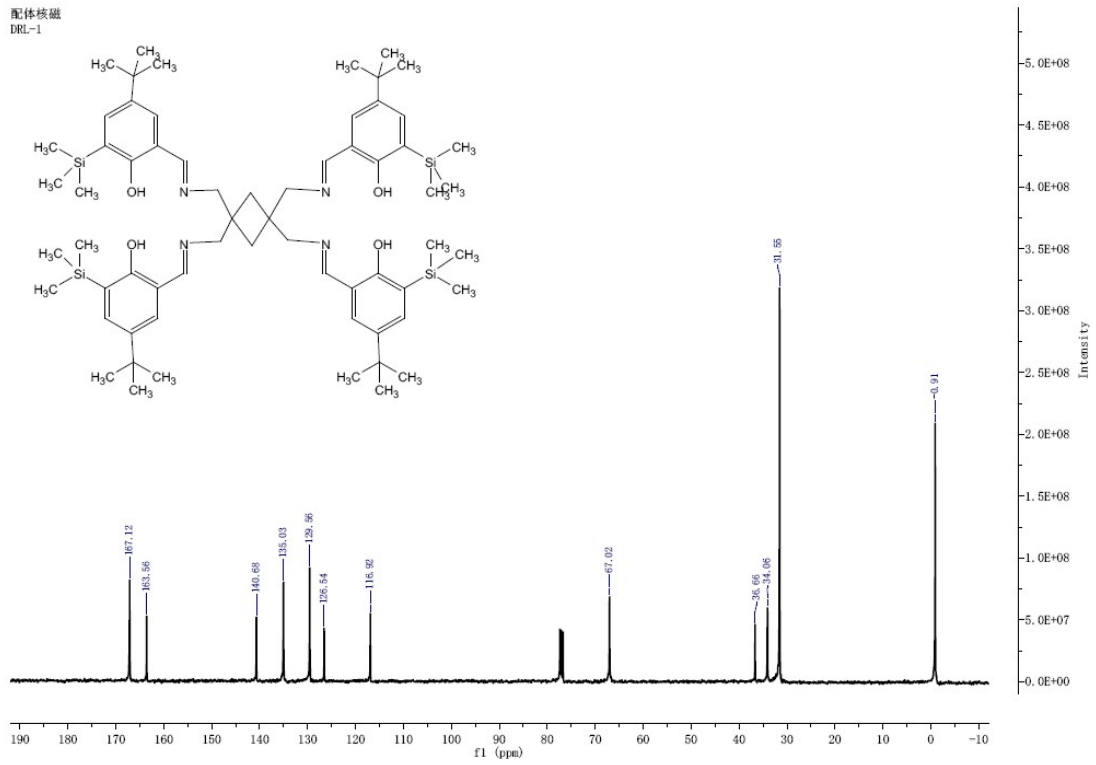

Figure S9-(3). ^{13}C NMR spectrum of **L^{3}**.

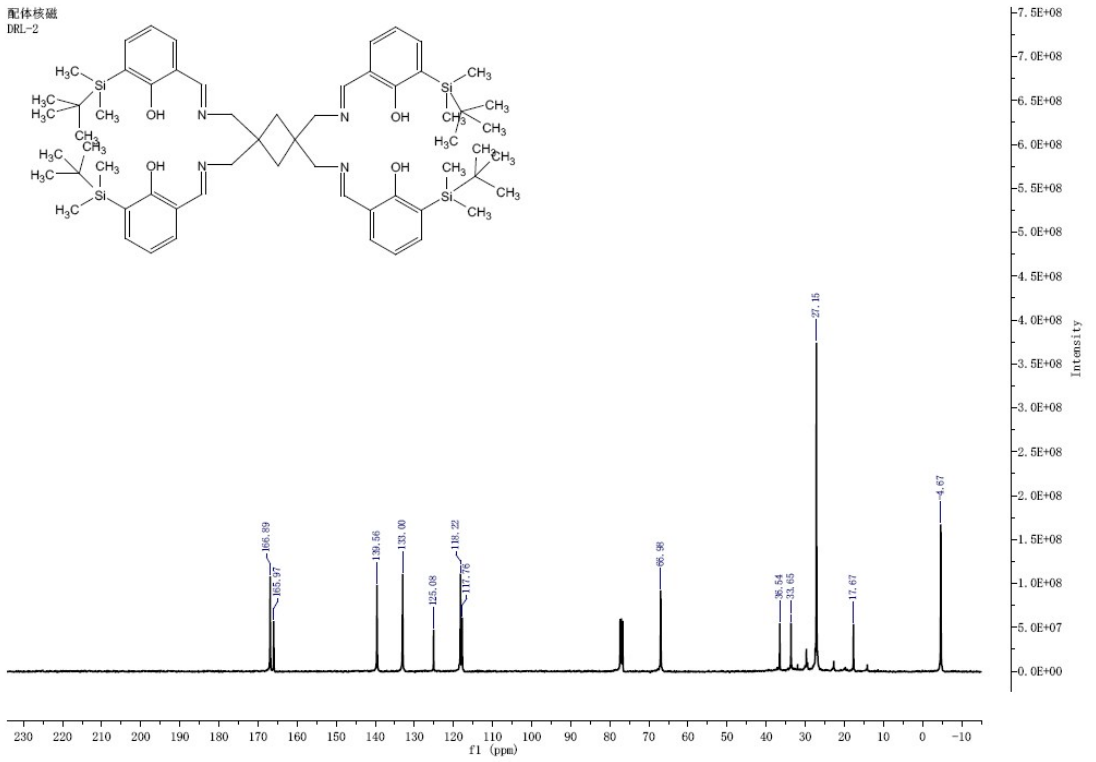

Figure S9-(4). ^{13}C NMR spectrum of **L^{4}**.

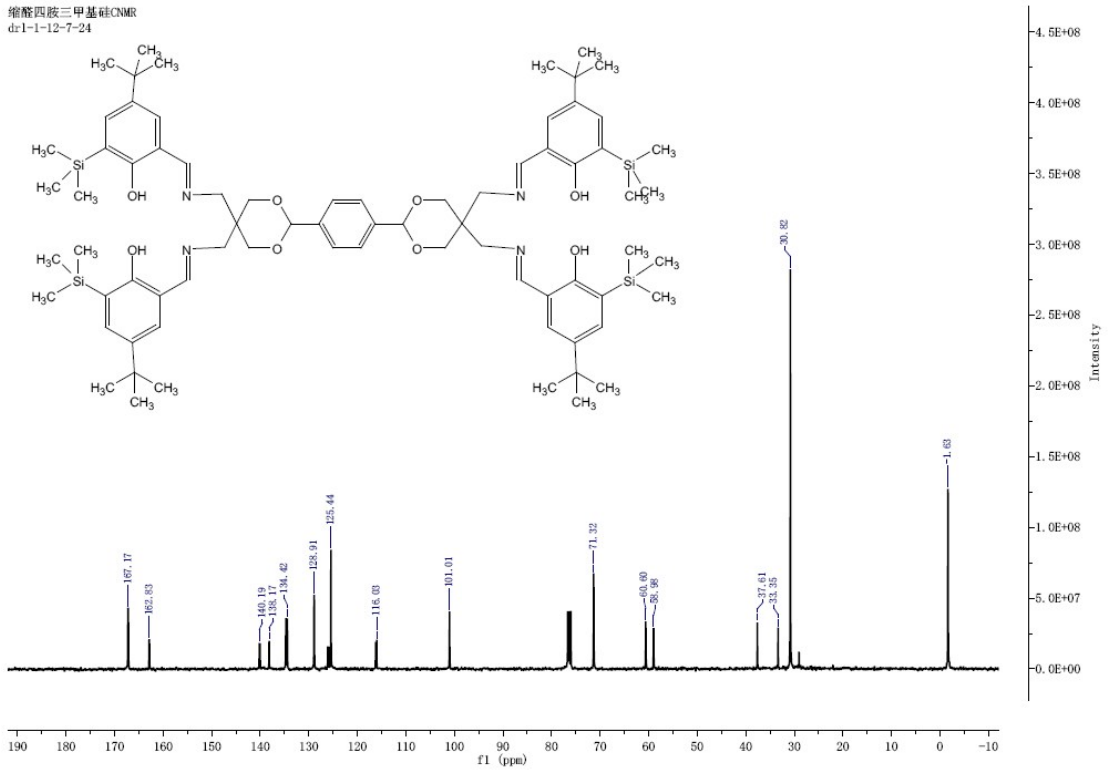

Figure S9-(5). ^{13}C NMR spectrum of **L^5**.

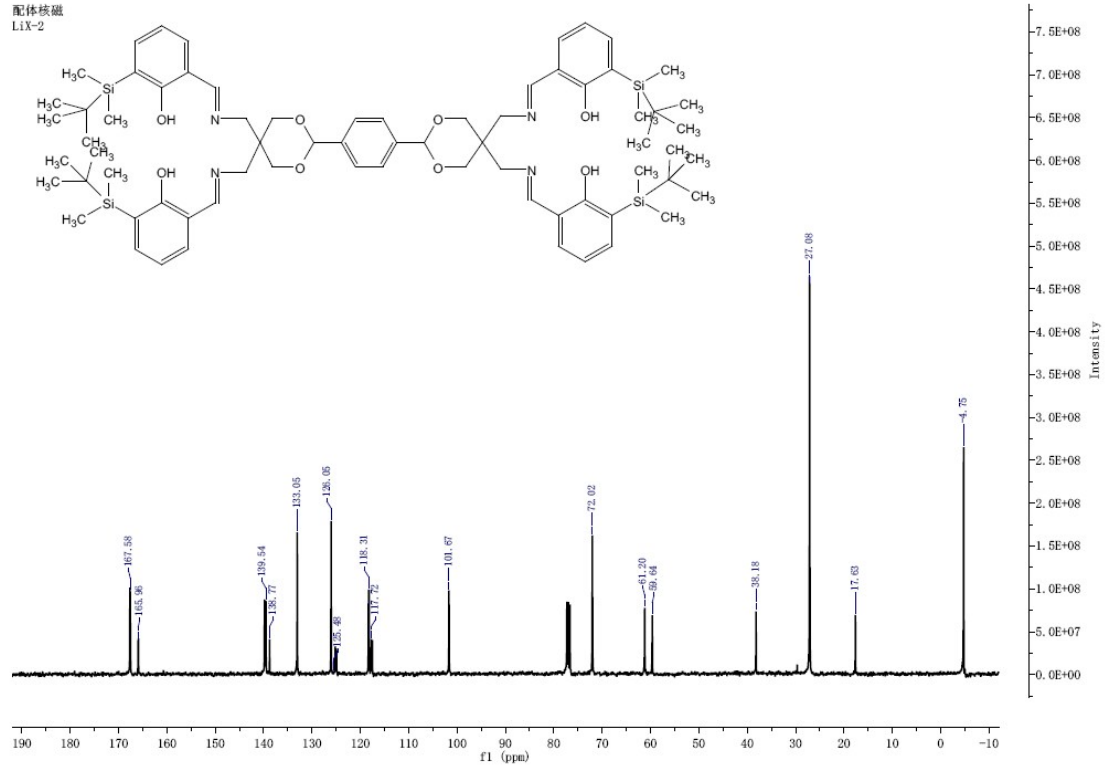

Figure S9-(6). ^{13}C NMR spectrum of **L^6**.

Figure S10-(1-6). HRMS spectra of **L[1]** -**L[6]**. Mono-peaks were found in spectra of **S10-(1), S10-(3)** and **S10-(5),** respectively, which were attributed to $[L^1+H]^+$, $[L^3+H]^+$ and $[L^5+H]^+$, respectively. Two peaks were found in each spectrum of **S10-(2), S10-(4)** and **S10-(6)**. The main peaks were attributed to $[L^2+H]^+$, $[L^4+H]^+$ and $[L^6+H]^+$. And the secondary peaks were attributed to the residuces of $[L^2-57)]^+$, $[L^4-57]^+$ and $[L^6-57]^+$, which were originated directly from the molecular ion by loss of a tert-butyl group $[C(CH_3)_3]^+$. Similar results were reported in the literature. [1-4]

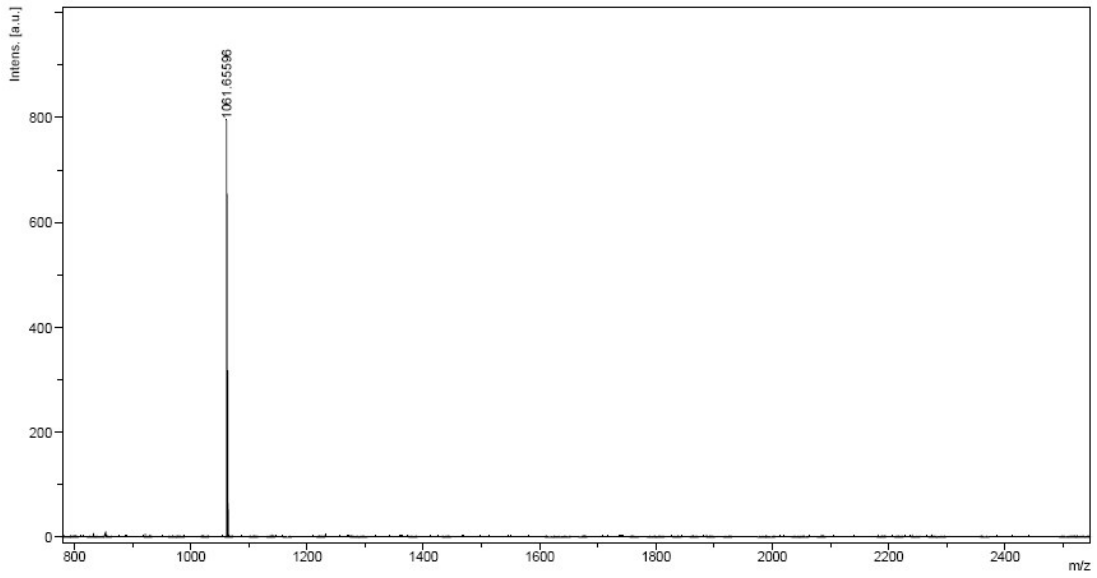

Figure S10-(1). HRMS spectrum of **L[1]**.

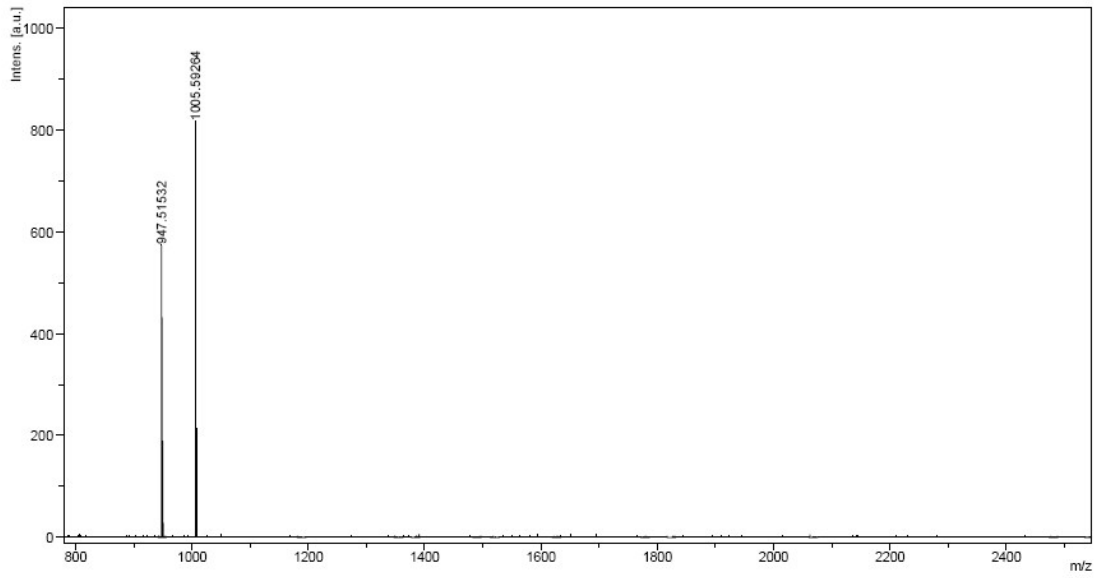

Figure S10-(2). HRMS spectrum of **L[2]**.

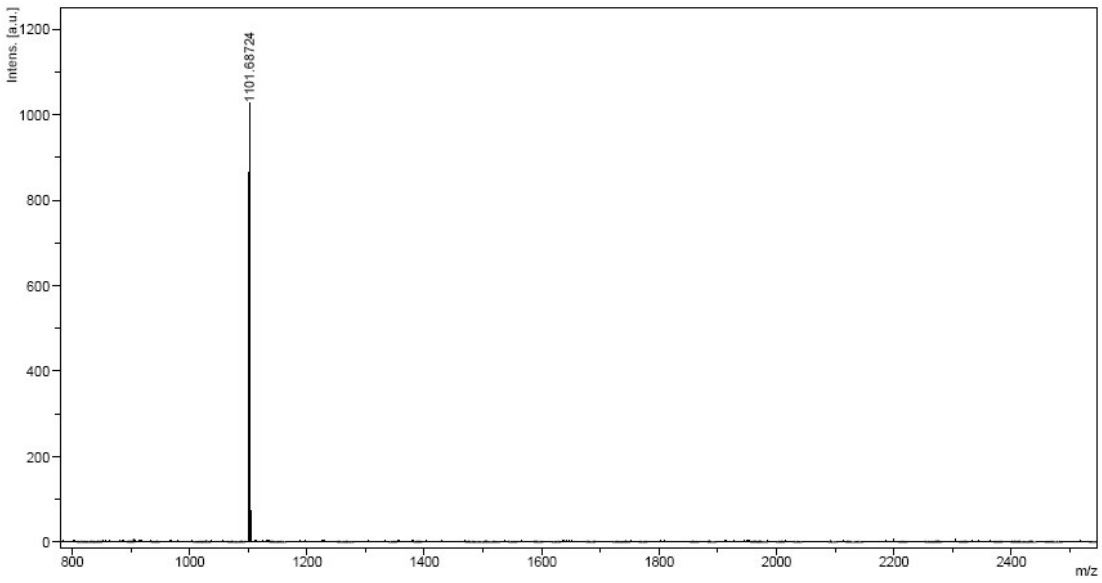

Figure S10-(3). HRMS spectrum of $\mathbf{L^3}$.

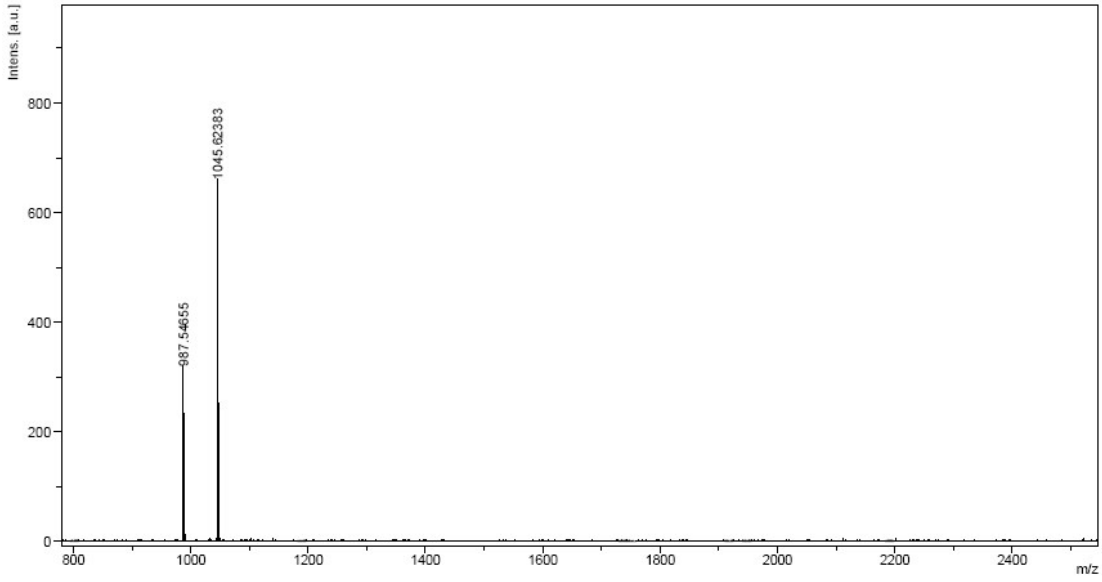

Figure S10-(4). HRMS spectrum of $\mathbf{L^4}$.

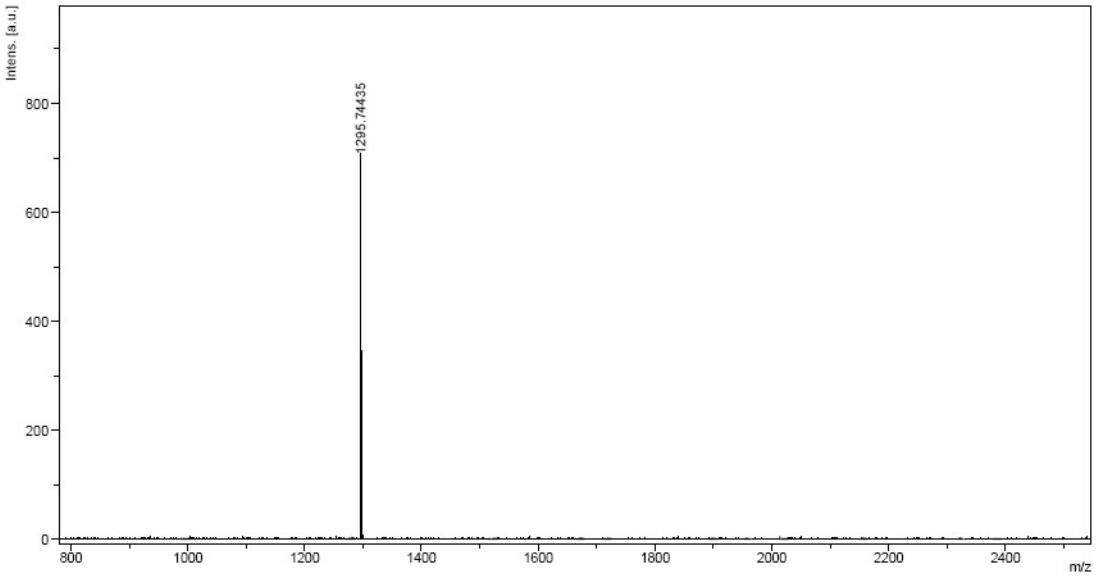

Figure S10-(5). HRMS spectrum of $\mathbf{L^5}$.

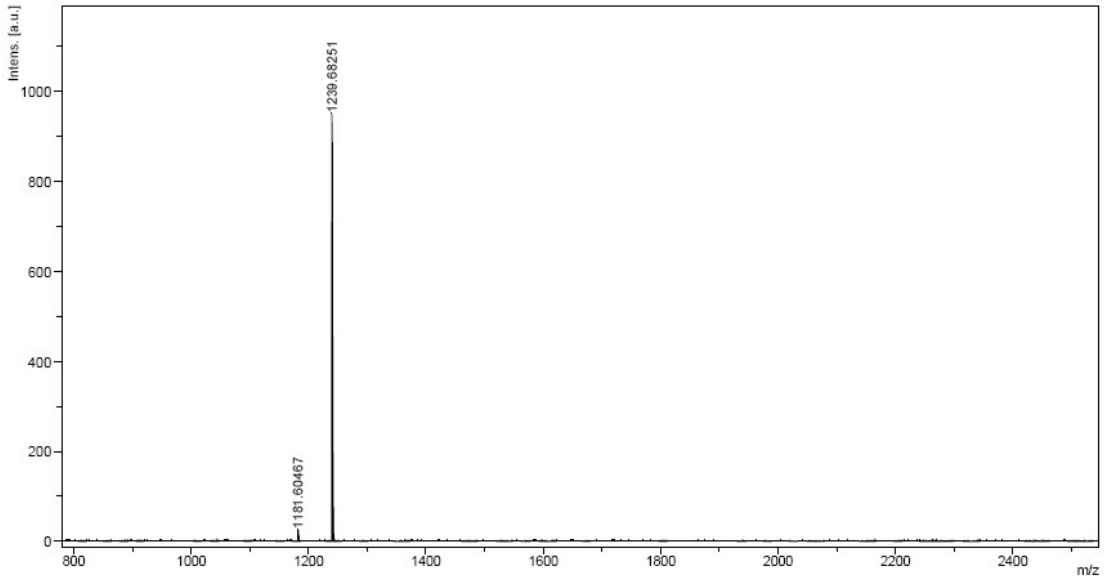

Figure S10-(6). HRMS spectrum of $\mathbf{L^6}$.

Figure S11-(1-6). ^{1}H NMR spectra of complexes **1a -6a**.

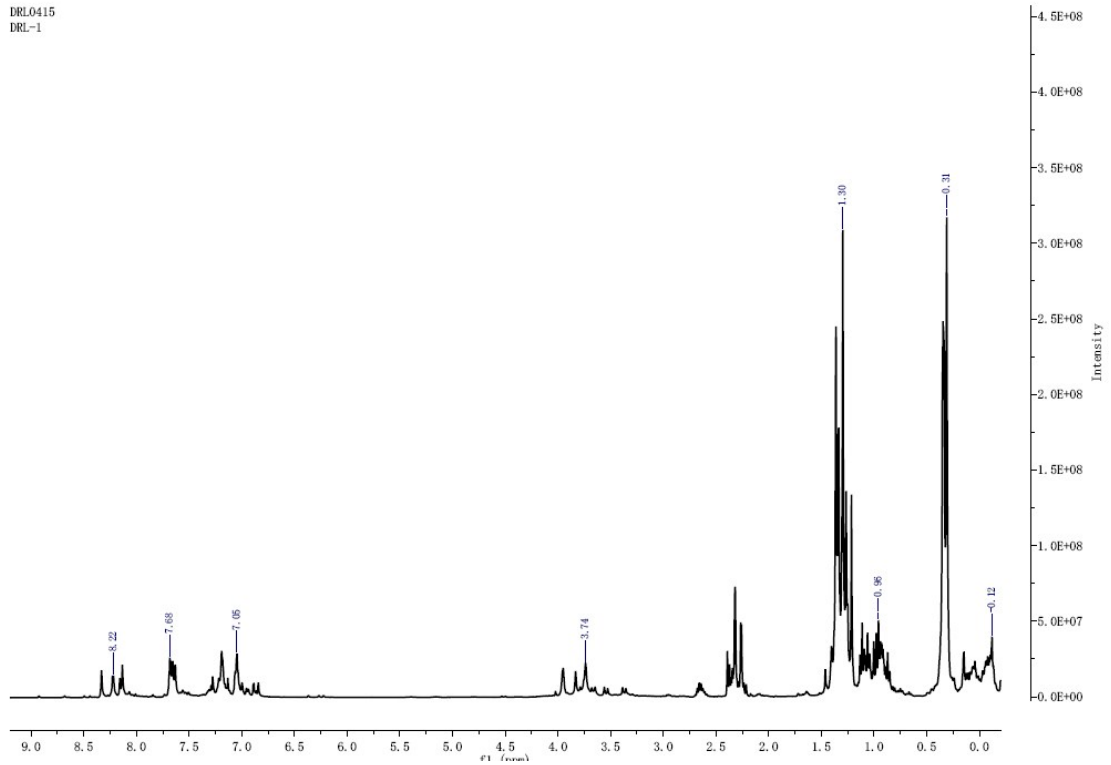

Figure S11-(1). ^{1}H NMR spectrum of complex **1a.**

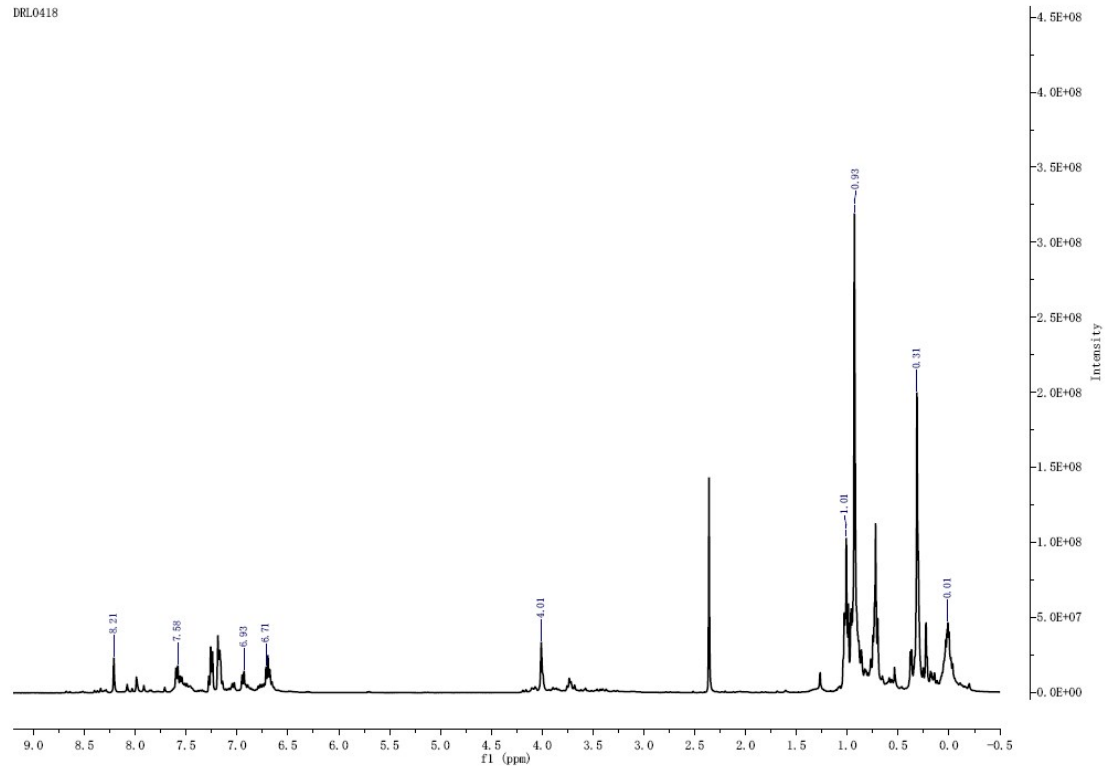

Figure S11-(2). ^{1}H NMR spectrum of complex **2a.**

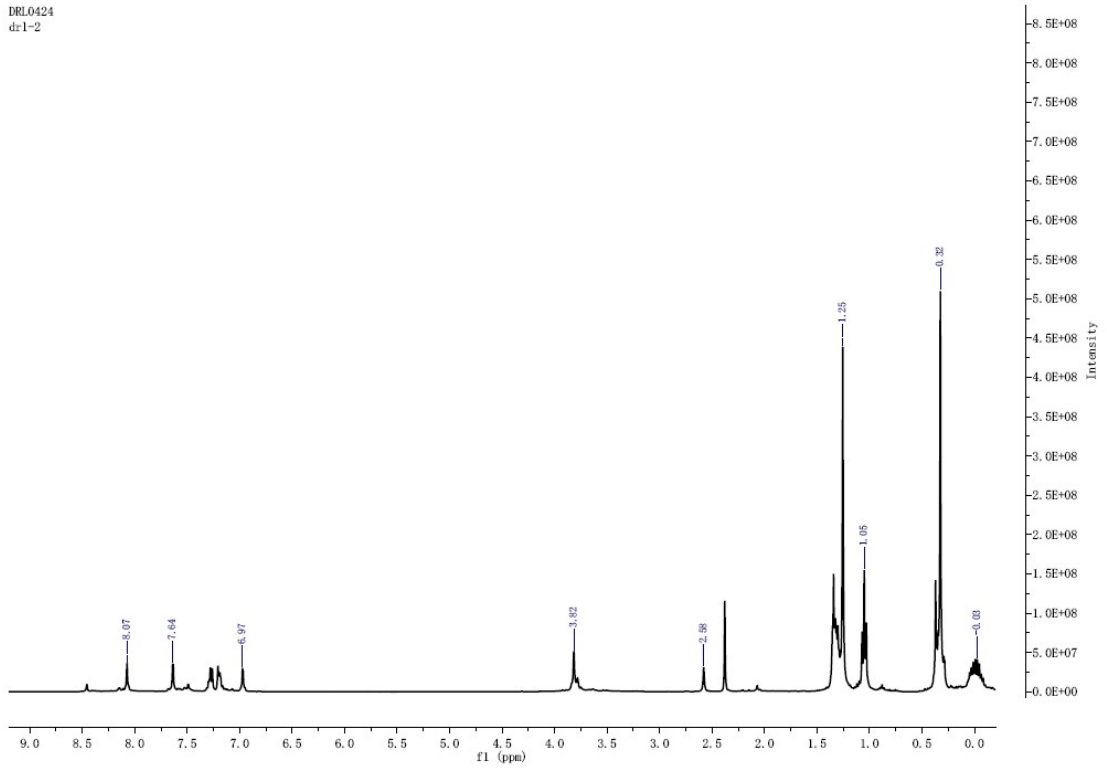

Figure S11-(3). ^{1}H NMR spectrum of complex **3a.**

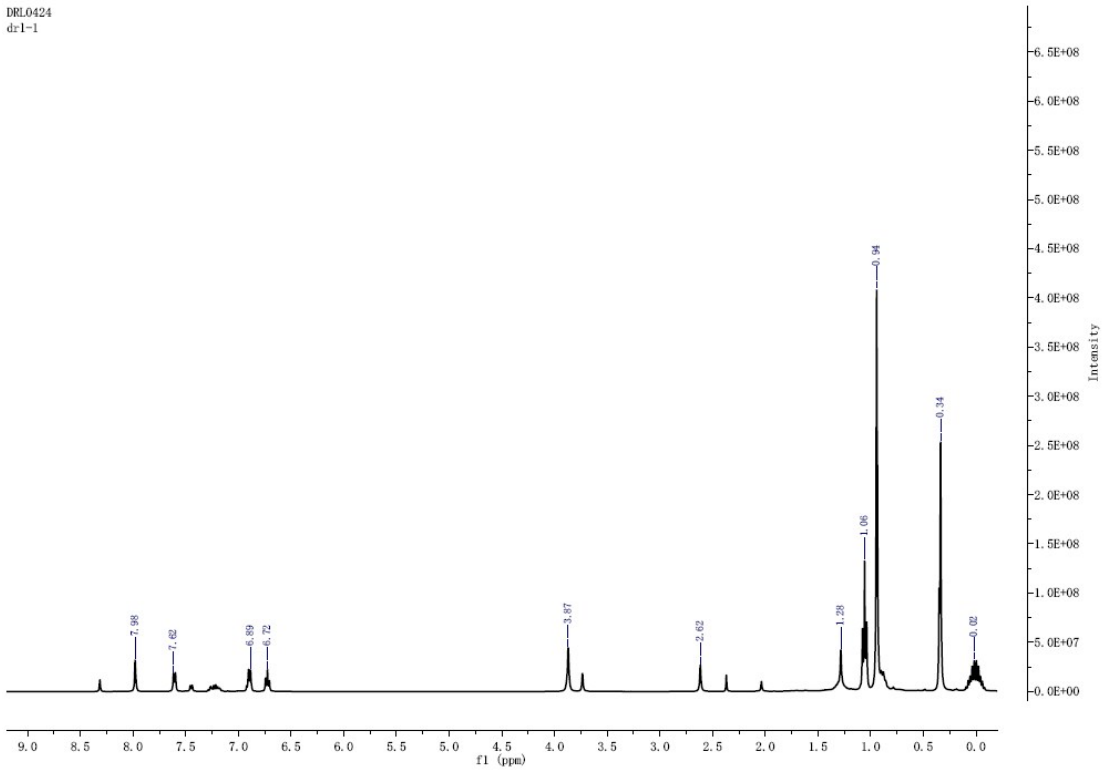

Figure S11-(4). ^{1}H NMR spectrum of complex **4a.**

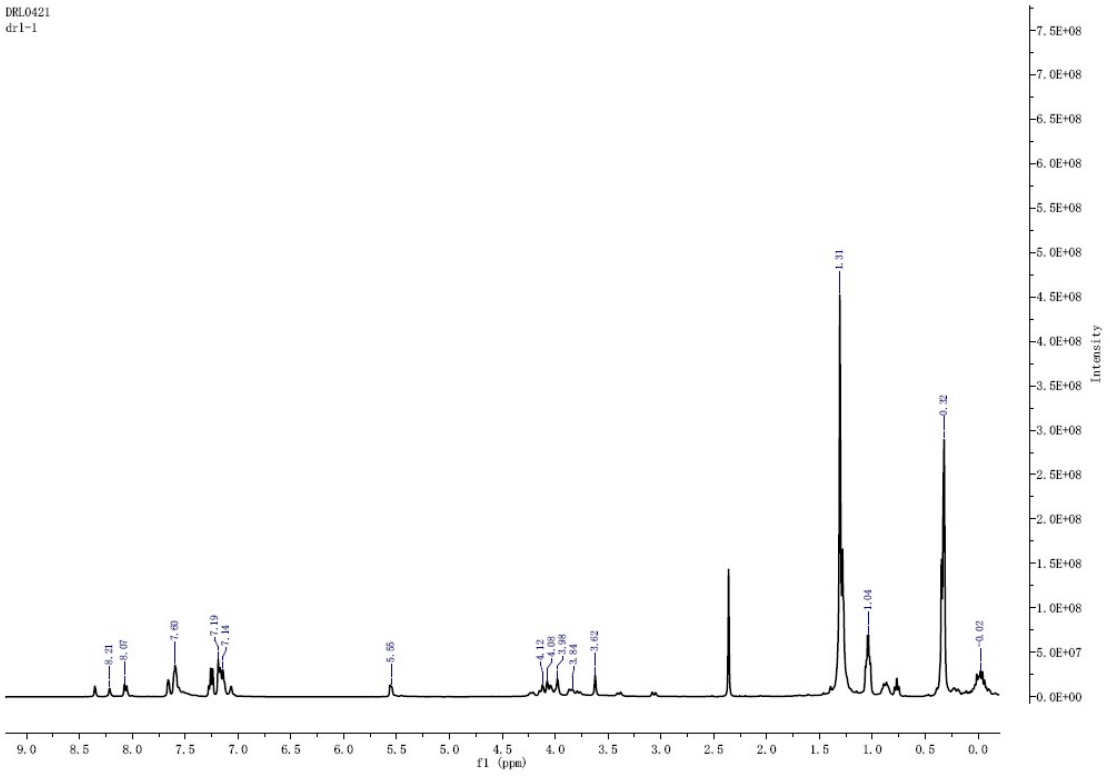

Figure S11-(5). ^{1}H NMR spectrum of complex **5a.**

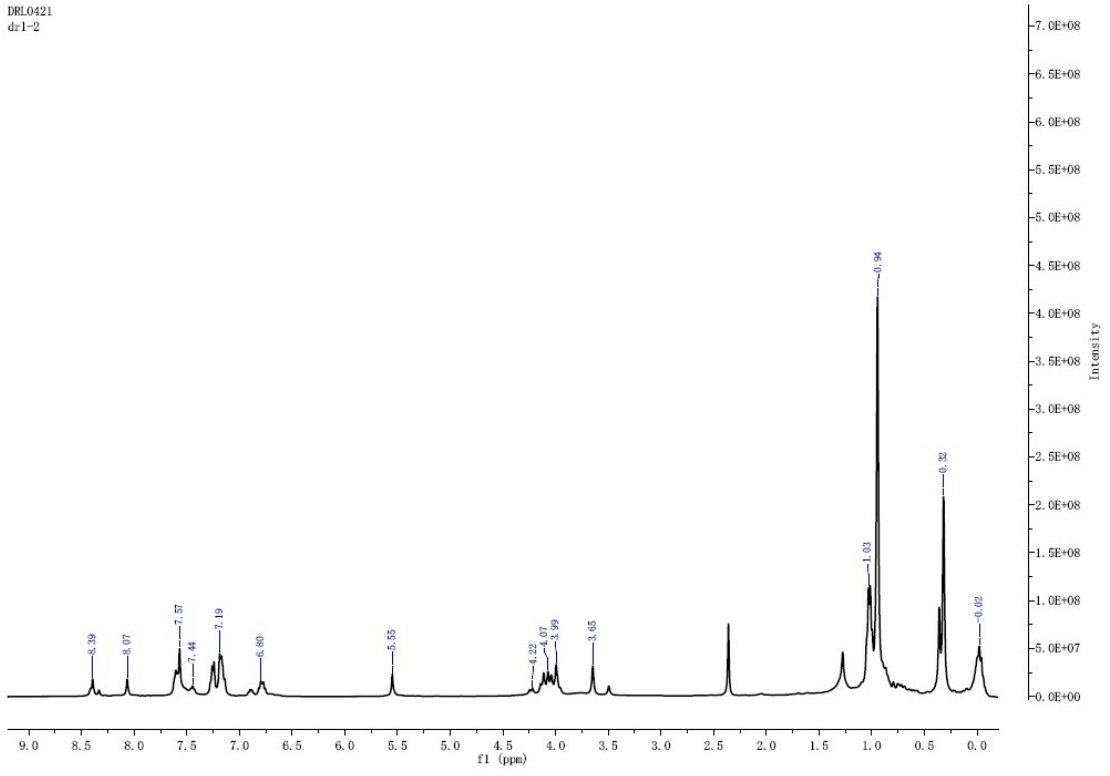

Figure S11-(6). ^{1}H NMR spectrum of complex **6a.**

Figure S12-(1-6). ^{13}C NMR spectra of complexes **1a -6a**.

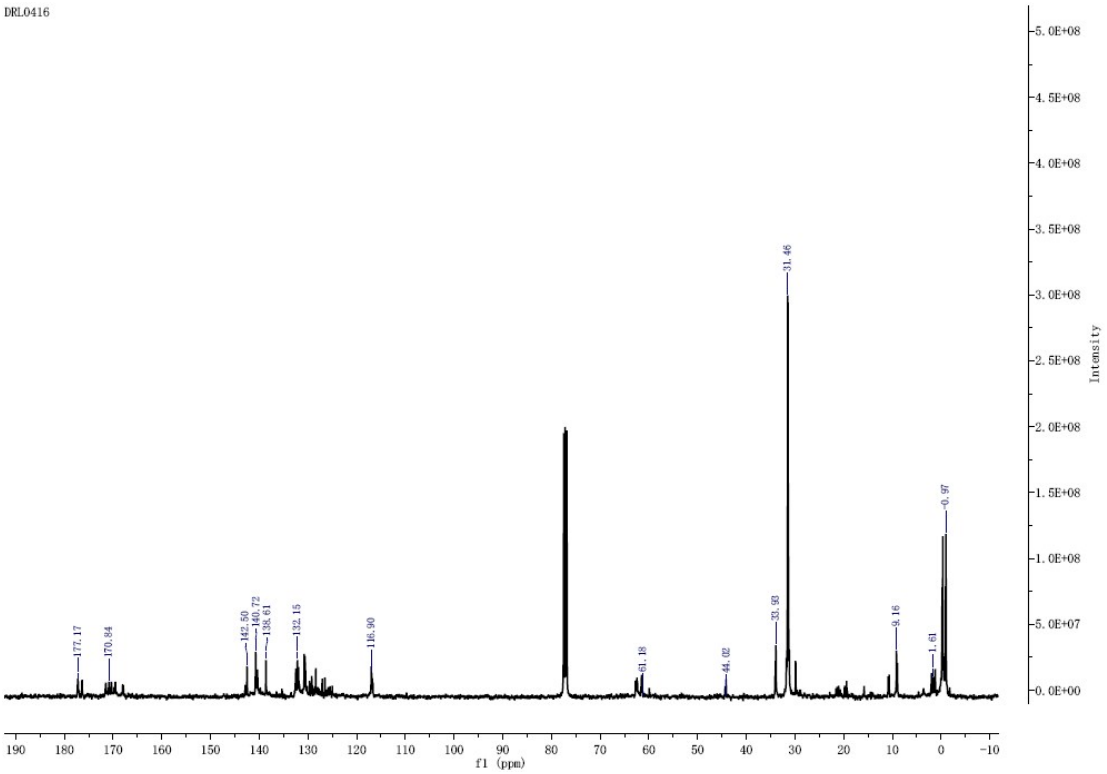

Figure S12-(1). ^{13}C NMR spectrum of complex **1a**.

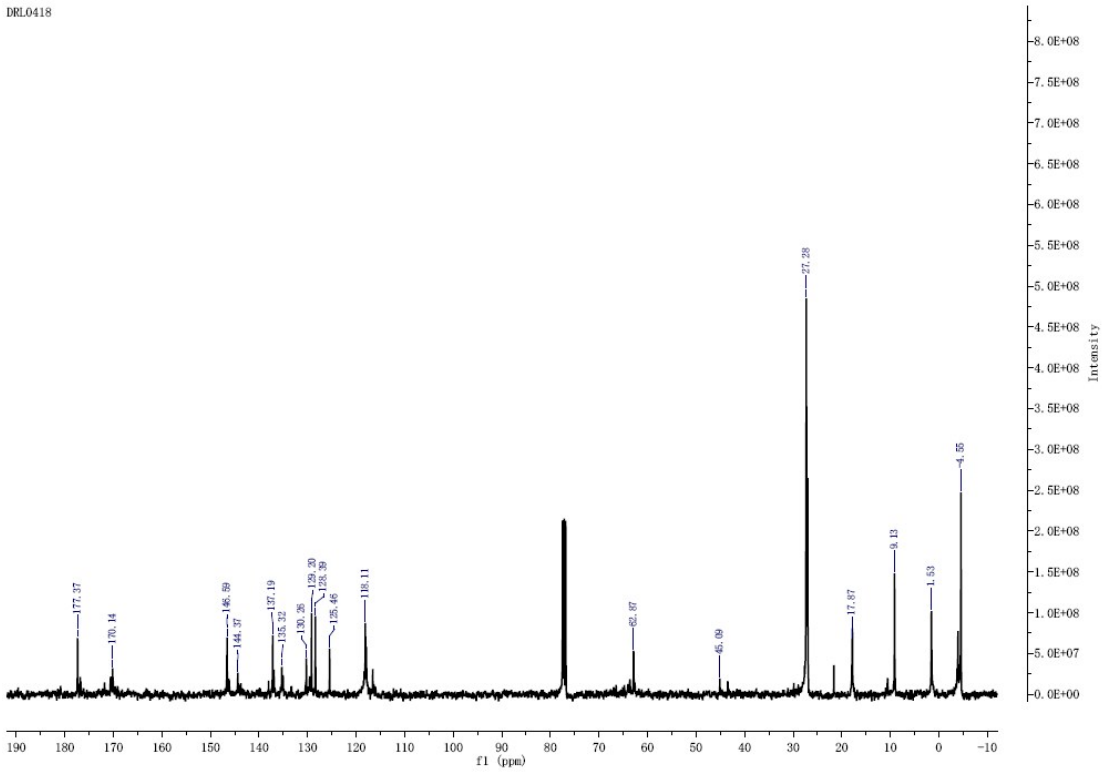

Figure S12-(2). ^{13}C NMR spectrum of complex **2a**.

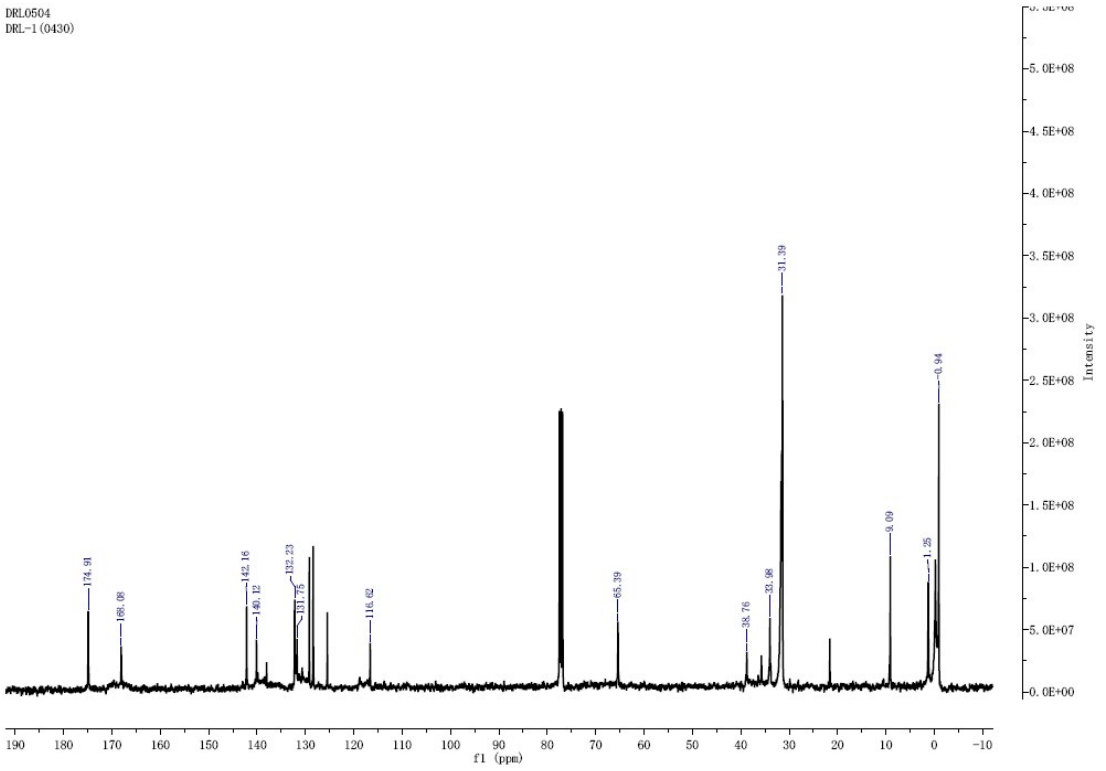

Figure S12-(3). ^{13}C NMR spectrum of complex **3a**.

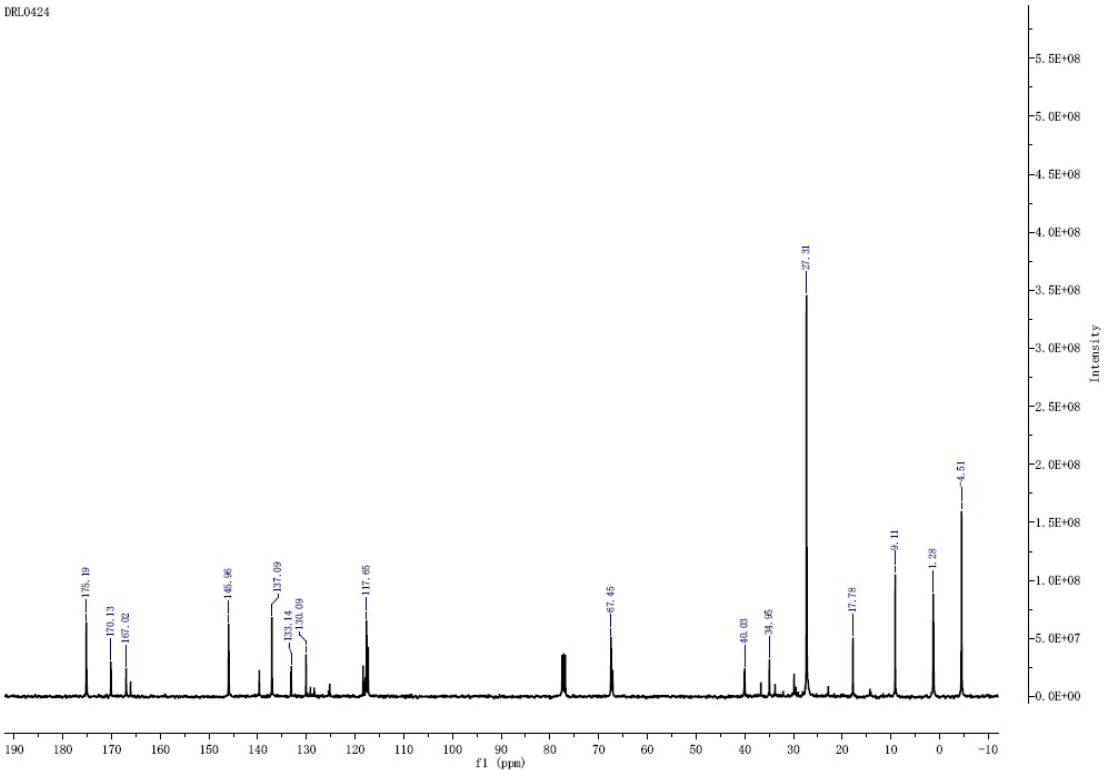

Figure S12-(4). ^{13}C NMR spectrum of complex **4a**.

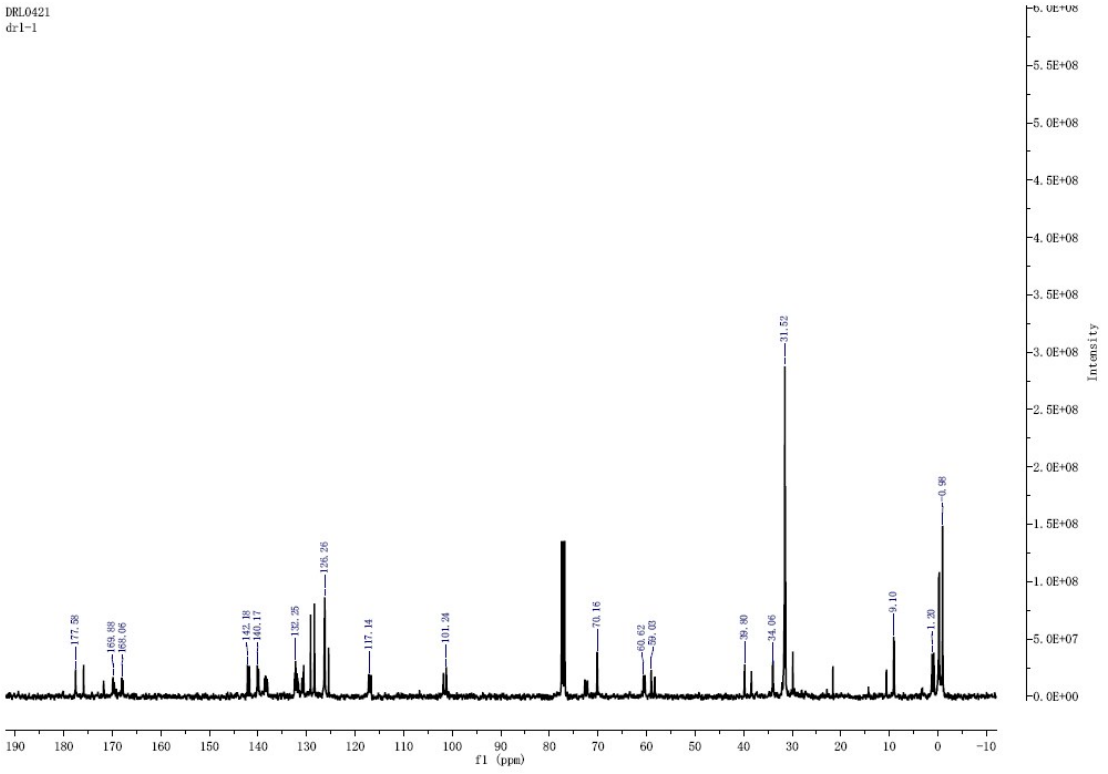

Figure S12-(5). ^{13}C NMR spectrum of complex **5a**.

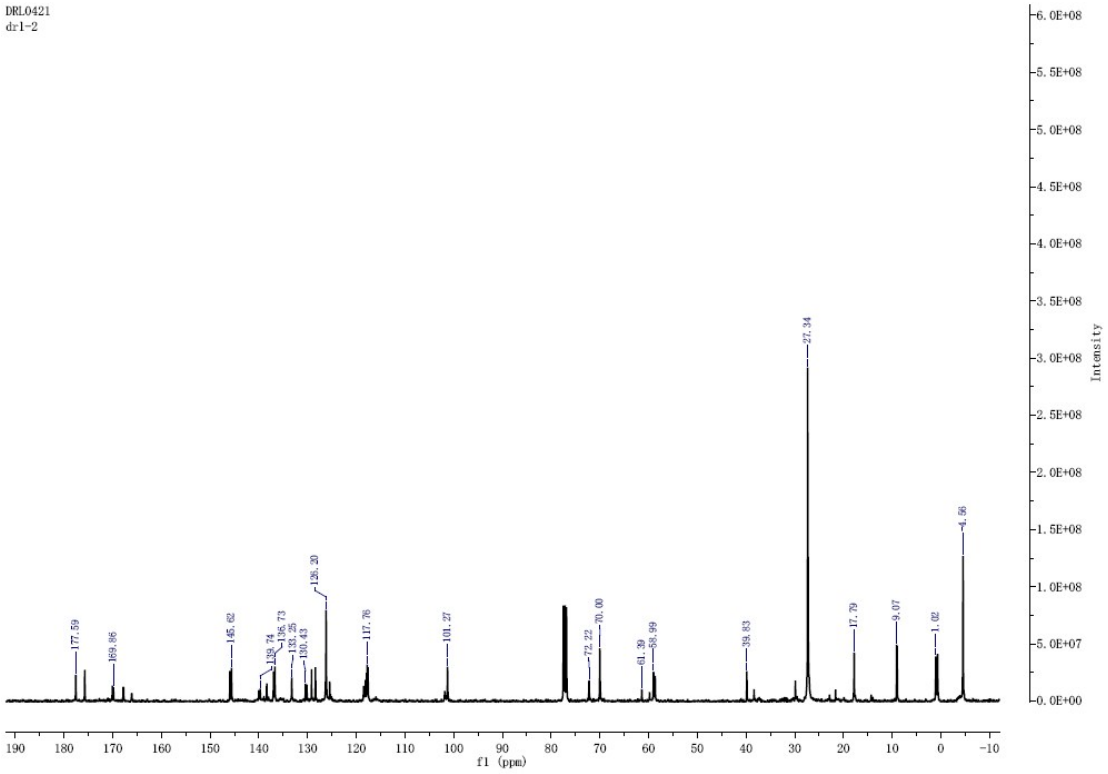

Figure S12-(6). ^{13}C NMR spectrum of complex **6a**.

Table S1. Copolymerisation data of rac-LA/ε-CL with complex **2a** [a].

Entry	[rac-LA]:[ε-CL] (mol)[b]	LA/CL in copolymers [c]	$M_{n(calcd)}$ [d][10^3]	$M_{n(GPC)}$ [e][10^3]	PDI[e]
1	90:10	88:12	1.40	2.02	1.31
2	80:20	77:23	1.37	1.77	1.34
3	70:30	68:32	1.34	1.99	1.49
4	60:40	57:43	1.31	1.97	1.58
5	50:50	49:51	1.29	1.94	1.66
6	40:60	37:63	1.25	1.92	1.36
7	30:70	26:74	1.22	1.99	1.36
8	20:80	17:83	1.19	2.01	1.39
9	10:90	7:93	1.16	1.95	1.33

[a] The polymerisations were carried out in toluene solution. $[M]_0$:[I] =100:1, $[M]_0=[LA]_0+[\varepsilon\text{-CL}]_0$=0.5 mol/L. [b] Feed ratio in mole. [c] CL/LA mole ratio in the copolymer measured by ^{1}H NMR spectra. [d] $M_{n(calcd)}$= [(M/I)×(percentage of LA units)×(mol wt of LA)]+[(M/I)×(percentage of CL units)×(mol wt of ε-CL)], percentage of LA units and CL units were obtained according to the CL/LA mole ratio in the copolymer. [e] Obtained from GPC analysis and calibrated against polystyrene standard. The true value of *Mn* could be calculated according to formula *Mn* = [0.58×(percentage of LA units)+0.56×(percentage of CL units)] ×$Mn_{GPC.}$

References

[1] S. Casal, E. Mendes, J.O. Fernandes, M. Oliveira, M.A. Ferreira, Analysis of heterocyclic aromatic amines in foods by gas chromatography-mass spectrometry as their tert.-butyldimethyl silyl derivatives, J. Chromatogr. A, 1040 (2004) 105-114.

[2] i.K.B. R.P. Evershed, J.M. Halket (Eds.), Handbook of derivatives for chromatography, Wiley, Chichester, (1993) 50-107.

[3] H.J.C. Dasneves, A.M.P. Vasconcelos, Capillary gas-chromatography of amino-acids, including asparagine and glutamine sensitive gas-chromatographic mass-spectrometric and selected ion monitoring gas-chromatographic mass-spectrometric detection of the N,O(S)-tert-butyldimethyl silyl derivatives, J. Chromatography. 392 (1987) 249-258.

[4] C.J. Biermann, C.M. Kinoshita, J.A. Marlett, R.D. Steele, Analysis of amino-acids as tert-butyldimethyl silyl derivatives by gas-chromattography, J. Chromatography, 357 (1986) 330-334.